

Measurement of azimuthal asymmetries in inclusive charged dipion production in e^+e^- annihilations at $\sqrt{s} = 3.65$ GeV

M. Ablikim¹, M. N. Achasov^{9,f}, X. C. Ai¹, O. Albayrak⁵, M. Albrecht⁴, D. J. Ambrose⁴⁴, A. Amoroso^{49A,49C}, F. F. An¹, Q. An^{46,a}, J. Z. Bai¹, R. Baldini Ferroli^{20A}, Y. Ban³¹, D. W. Bennett¹⁹, J. V. Bennett⁵, M. Bertani^{20A}, D. Bettoni^{21A}, J. M. Bian⁴³, F. Bianchi^{49A,49C}, E. Boger^{23,d}, I. Boyko²³, R. A. Briere⁵, H. Cai⁵¹, X. Cai^{1,a}, O. Cakir^{40A,b}, A. Calcaterra^{20A}, G. F. Cao¹, S. A. Cetin^{40B}, J. F. Chang^{1,a}, G. Chelkov^{23,d,e}, G. Chen¹, H. S. Chen¹, H. Y. Chen², J. C. Chen¹, M. L. Chen^{1,a}, S. J. Chen²⁹, X. Chen^{1,a}, X. R. Chen²⁶, Y. B. Chen^{1,a}, H. P. Cheng¹⁷, X. K. Chu³¹, G. Cibinetto^{21A}, H. L. Dai^{1,a}, J. P. Dai³⁴, A. Dbeyssi¹⁴, D. Dedovich²³, Z. Y. Deng¹, A. Denig²², I. Denysenko²³, M. Destefanis^{49A,49C}, F. De Mori^{49A,49C}, Y. Ding²⁷, C. Dong³⁰, J. Dong^{1,a}, L. Y. Dong¹, M. Y. Dong^{1,a}, S. X. Du⁵³, P. F. Duan¹, E. E. Eren^{40B}, J. Z. Fan³⁹, J. Fang^{1,a}, S. S. Fang¹, X. Fang^{46,a}, Y. Fang¹, L. Fava^{49B,49C}, F. Feldbauer²², G. Felici^{20A}, C. Q. Feng^{46,a}, E. Fioravanti^{21A}, M. Fritsch^{14,22}, C. D. Fu¹, Q. Gao¹, X. Y. Gao², Y. Gao³⁹, Z. Gao^{46,a}, I. Garzia^{21A}, K. Goetzen¹⁰, W. X. Gong^{1,a}, W. Gradl²², M. Greco^{49A,49C}, M. H. Gu^{1,a}, Y. T. Gu¹², Y. H. Guan¹, A. Q. Guo¹, L. B. Guo²⁸, Y. Guo¹, Y. P. Guo²², Z. Haddadi²⁵, A. Hafner²², S. Han⁵¹, J. Q. Hao¹⁵, F. A. Harris⁴², K. L. He¹, X. Q. He⁴⁵, T. Held⁴, Y. K. Heng^{1,a}, Z. L. Hou¹, C. Hu²⁸, H. M. Hu¹, X. F. Hu^{49A,49C}, T. Hu^{1,a}, Y. Hu¹, G. M. Huang⁶, G. S. Huang^{46,a}, J. S. Huang¹⁵, X. T. Huang³³, Y. Huang²⁹, T. Hussain⁴⁸, Q. Ji¹, Q. P. Ji³⁰, X. B. Ji¹, X. L. Ji^{1,a}, L. W. Jiang⁵¹, X. S. Jiang^{1,a}, X. Y. Jiang³⁰, J. B. Jiao³³, Z. Jiao¹⁷, D. P. Jin^{1,a}, S. Jin¹, T. Johansson⁵⁰, A. Julin⁴³, N. Kalantar-Nayestanaki²⁵, X. L. Kang¹, X. S. Kang³⁰, M. Kavatsyuk²⁵, B. C. Ke⁵, P. Kiese²², R. Kliemt¹⁴, B. Kloss²², O. B. Kolcu^{40B,i}, B. Kopf⁴, M. Kornicer⁴², W. Kühn²⁴, A. Kupsc⁵⁰, J. S. Lange²⁴, M. Lara¹⁹, P. Larin¹⁴, C. Leng^{49C}, C. Li⁵⁰, Cheng Li^{46,a}, D. M. Li⁵³, F. Li^{1,a}, F. Y. Li³¹, G. Li¹, H. B. Li¹, J. C. Li¹, Jin Li³², K. Li³³, K. Li³³, Lei Li³, P. R. Li⁴¹, T. Li³³, W. D. Li¹, W. G. Li¹, X. L. Li³³, X. M. Li¹², X. N. Li^{1,a}, X. Q. Li³⁰, Z. B. Li³⁸, H. Liang^{46,a}, Y. F. Liang³⁶, Y. T. Liang²⁴, G. R. Liao¹¹, D. X. Lin¹⁴, B. J. Liu¹, C. X. Liu¹, F. H. Liu³⁵, Fang Liu¹, Feng Liu⁶, H. B. Liu¹², H. H. Liu¹⁶, H. H. Liu¹, H. M. Liu¹, J. Liu¹, J. B. Liu^{46,a}, J. P. Liu⁵¹, J. Y. Liu¹, K. Liu³⁹, K. Y. Liu²⁷, L. D. Liu³¹, P. L. Liu^{1,a}, Q. Liu⁴¹, S. B. Liu^{46,a}, X. Liu²⁶, Y. B. Liu³⁰, Z. A. Liu^{1,a}, Zhiqing Liu²², H. Loehner²⁵, X. C. Lou^{1,a,h}, H. J. Lu¹⁷, J. G. Lu^{1,a}, Y. Lu¹, Y. P. Lu^{1,a}, C. L. Luo²⁸, M. X. Luo⁵², T. Luo⁴², X. L. Luo^{1,a}, X. R. Lyu⁴¹, F. C. Ma²⁷, H. L. Ma¹, L. L. Ma³³, Q. M. Ma¹, T. Ma¹, X. N. Ma³⁰, X. Y. Ma^{1,a}, F. E. Maas¹⁴, M. Maggiora^{49A,49C}, Y. J. Mao³¹, Z. P. Mao¹, S. Marcello^{49A,49C}, J. G. Messchendorp²⁵, J. Min^{1,a}, R. E. Mitchell¹⁹, X. H. Mo^{1,a}, Y. J. Mo⁶, C. Morales Morales¹⁴, K. Moriya¹⁹, N. Yu. Muchnoi^{9,f}, H. Muramatsu⁴³, Y. Nefedov²³, F. Nerling¹⁴, I. B. Nikolaev^{9,f}, Z. Ning^{1,a}, S. Nisar⁸, S. L. Niu^{1,a}, X. Y. Niu¹, S. L. Olsen³², Q. Ouyang^{1,a}, S. Pacetti^{20B}, P. Patteri^{20A}, M. Pelizaeus⁴, H. P. Peng^{46,a}, K. Peters¹⁰, J. Pettersson⁵⁰, J. L. Ping³², R. G. Ping¹, R. Poling⁴³, V. Prasad¹, M. Qi²⁹, S. Qian^{1,a}, C. F. Qiao⁴¹, L. Q. Qin³³, N. Qin⁵¹, X. S. Qin¹, Z. H. Qin^{1,a}, J. F. Qiu¹, K. H. Rashid⁴⁸, C. F. Redmer²², M. Ripka²², G. Rong¹, Ch. Rosner¹⁴, X. D. Ruan¹², V. Santoro^{21A}, A. Sarantsev^{23,g}, M. Savrie^{21B}, K. Schoenning⁵⁰, S. Schumann²², W. Shan³¹, M. Shao^{46,a}, C. P. Shen², P. X. Shen³⁰, X. Y. Shen¹, H. Y. Sheng¹, W. M. Song¹, X. Y. Song¹, S. Sosio^{49A,49C}, S. Spataro^{49A,49C}, G. X. Sun¹, J. F. Sun¹⁵, S. S. Sun¹, Y. J. Sun^{46,a}, Y. Z. Sun¹, Z. J. Sun^{1,a}, Z. T. Sun¹⁹, C. J. Tang³⁶, X. Tang¹, I. Tapan^{40C}, E. H. Thorndike⁴⁴, M. Tiemens²⁵, M. Ullrich²⁴, I. Uman^{40B}, G. S. Varner⁴², B. Wang³⁰, D. Wang³¹, D. Y. Wang³¹, K. Wang^{1,a}, L. L. Wang¹, L. S. Wang¹, M. Wang³³, P. Wang¹, P. L. Wang¹, S. G. Wang³¹, W. Wang^{1,a}, X. F. Wang³⁹, Y. D. Wang¹⁴, Y. F. Wang^{1,a}, Y. Q. Wang²², Z. Wang^{1,a}, Z. G. Wang^{1,a}, Z. H. Wang^{46,a}, Z. Y. Wang¹, T. Weber²², D. H. Wei¹¹, J. B. Wei³¹, P. Weidenkaff²², S. P. Wen¹, U. Wiedner⁴, M. Wolke⁵⁰, L. H. Wu¹, Z. Wu^{1,a}, L. G. Xia³⁹, Y. Xia¹⁸, D. Xiao¹, H. Xiao⁴⁷, Z. J. Xiao²⁸, Y. G. Xie^{1,a}, Q. L. Xiu^{1,a}, G. F. Xu¹, L. Xu¹, Q. J. Xu¹³, X. P. Xu³⁷, L. Yan^{46,a}, W. B. Yan^{46,a}, W. C. Yan^{46,a}, Y. H. Yan¹⁸, H. J. Yang³⁴, H. X. Yang¹, L. Yang⁵¹, Y. Yang⁶, Y. X. Yang¹¹, M. Ye^{1,a}, M. H. Ye⁷, J. H. Yin¹, B. X. Yu^{1,a}, C. X. Yu³⁰, J. S. Yu²⁶, C. Z. Yuan¹, W. L. Yuan²⁹, Y. Yuan¹, A. Yuncu^{40B,c}, A. A. Zafar⁴⁸, A. Zallo^{20A}, Y. Zeng¹⁸, B. X. Zhang¹, B. Y. Zhang^{1,a}, C. Zhang²⁹, C. C. Zhang¹, D. H. Zhang¹, H. H. Zhang³⁸, H. Y. Zhang^{1,a}, J. J. Zhang¹, J. L. Zhang¹, J. Q. Zhang¹, J. W. Zhang^{1,a}, J. Y. Zhang¹, J. Z. Zhang¹, K. Zhang¹, L. Zhang¹, X. Y. Zhang³³, Y. Zhang¹, Y. N. Zhang⁴¹, Y. H. Zhang^{1,a}, Y. T. Zhang^{46,a}, Yu Zhang⁴¹, Z. H. Zhang⁶, Z. P. Zhang⁴⁶, Z. Y. Zhang⁵¹, G. Zhao¹, J. W. Zhao^{1,a}, J. Y. Zhao¹, J. Z. Zhao^{1,a}, Lei Zhao^{46,a}, Ling Zhao¹, M. G. Zhao³⁰, Q. Zhao¹, Q. W. Zhao¹, S. J. Zhao⁵³, T. C. Zhao¹, Y. B. Zhao^{1,a}, Z. G. Zhao^{46,a}, A. Zhemchugov^{23,d}, B. Zheng⁴⁷, J. P. Zheng^{1,a}, W. J. Zheng³³, Y. H. Zheng⁴¹, B. Zhong²⁸, L. Zhou^{1,a}, X. Zhou⁵¹, X. K. Zhou^{46,a}, X. R. Zhou^{46,a}, X. Y. Zhou¹, K. Zhu¹, K. J. Zhu^{1,a}, S. Zhu¹, S. H. Zhu⁴⁵, X. L. Zhu³⁹, Y. C. Zhu^{46,a}, Y. S. Zhu¹, Z. A. Zhu¹, J. Zhuang^{1,a}, L. Zotti^{49A,49C}, B. S. Zou¹, J. H. Zou¹

(BESIII Collaboration)

¹ Institute of High Energy Physics, Beijing 100049, People's Republic of China

² Beihang University, Beijing 100191, People's Republic of China

³ Beijing Institute of Petrochemical Technology, Beijing 102617, People's Republic of China

⁴ Bochum Ruhr-University, D-44780 Bochum, Germany

⁵ Carnegie Mellon University, Pittsburgh, Pennsylvania 15213, USA

⁶ Central China Normal University, Wuhan 430079, People's Republic of China

⁷ China Center of Advanced Science and Technology, Beijing 100190, People's Republic of China

⁸ COMSATS Institute of Information Technology, Lahore, Defence Road, Off Raiwind Road, 54000 Lahore, Pakistan

⁹ G.I. Budker Institute of Nuclear Physics SB RAS (BINP), Novosibirsk 630090, Russia

¹⁰ GSI Helmholtzcentre for Heavy Ion Research GmbH, D-64291 Darmstadt, Germany

¹¹ Guangxi Normal University, Guilin 541004, People's Republic of China

- ¹² GuangXi University, Nanning 530004, People's Republic of China
- ¹³ Hangzhou Normal University, Hangzhou 310036, People's Republic of China
- ¹⁴ Helmholtz Institute Mainz, Johann-Joachim-Becher-Weg 45, D-55099 Mainz, Germany
- ¹⁵ Henan Normal University, Xinxiang 453007, People's Republic of China
- ¹⁶ Henan University of Science and Technology, Luoyang 471003, People's Republic of China
- ¹⁷ Huangshan College, Huangshan 245000, People's Republic of China
- ¹⁸ Hunan University, Changsha 410082, People's Republic of China
- ¹⁹ Indiana University, Bloomington, Indiana 47405, USA
- ²⁰ (A)INFN Laboratori Nazionali di Frascati, I-00044, Frascati, Italy; (B)INFN and University of Perugia, I-06100, Perugia, Italy
- ²¹ (A)INFN Sezione di Ferrara, I-44122, Ferrara, Italy; (B)University of Ferrara, I-44122, Ferrara, Italy
- ²² Johannes Gutenberg University of Mainz, Johann-Joachim-Becher-Weg 45, D-55099 Mainz, Germany
- ²³ Joint Institute for Nuclear Research, 141980 Dubna, Moscow region, Russia
- ²⁴ Justus Liebig University Giessen, II. Physikalisches Institut, Heinrich-Buff-Ring 16, D-35392 Giessen, Germany
- ²⁵ KVI-CART, University of Groningen, NL-9747 AA Groningen, The Netherlands
- ²⁶ Lanzhou University, Lanzhou 730000, People's Republic of China
- ²⁷ Liaoning University, Shenyang 110036, People's Republic of China
- ²⁸ Nanjing Normal University, Nanjing 210023, People's Republic of China
- ²⁹ Nanjing University, Nanjing 210093, People's Republic of China
- ³⁰ Nankai University, Tianjin 300071, People's Republic of China
- ³¹ Peking University, Beijing 100871, People's Republic of China
- ³² Seoul National University, Seoul, 151-747 Korea
- ³³ Shandong University, Jinan 250100, People's Republic of China
- ³⁴ Shanghai Jiao Tong University, Shanghai 200240, People's Republic of China
- ³⁵ Shanxi University, Taiyuan 030006, People's Republic of China
- ³⁶ Sichuan University, Chengdu 610064, People's Republic of China
- ³⁷ Soochow University, Suzhou 215006, People's Republic of China
- ³⁸ Sun Yat-Sen University, Guangzhou 510275, People's Republic of China
- ³⁹ Tsinghua University, Beijing 100084, People's Republic of China
- ⁴⁰ (A)Istanbul Aydin University, 34295 Sefakoy, Istanbul, Turkey; (B)Dogus University, 34722 Istanbul, Turkey; (C)Uludag University, 16059 Bursa, Turkey
- ⁴¹ University of Chinese Academy of Sciences, Beijing 100049, People's Republic of China
- ⁴² University of Hawaii, Honolulu, Hawaii 96822, USA
- ⁴³ University of Minnesota, Minneapolis, Minnesota 55455, USA
- ⁴⁴ University of Rochester, Rochester, New York 14627, USA
- ⁴⁵ University of Science and Technology Liaoning, Anshan 114051, People's Republic of China
- ⁴⁶ University of Science and Technology of China, Hefei 230026, People's Republic of China
- ⁴⁷ University of South China, Hengyang 421001, People's Republic of China
- ⁴⁸ University of the Punjab, Lahore-54590, Pakistan
- ⁴⁹ (A)University of Turin, I-10125, Turin, Italy; (B)University of Eastern Piedmont, I-15121, Alessandria, Italy; (C)INFN, I-10125, Turin, Italy
- ⁵⁰ Uppsala University, Box 516, SE-75120 Uppsala, Sweden
- ⁵¹ Wuhan University, Wuhan 430072, People's Republic of China
- ⁵² Zhejiang University, Hangzhou 310027, People's Republic of China
- ⁵³ Zhengzhou University, Zhengzhou 450001, People's Republic of China
- ^a Also at State Key Laboratory of Particle Detection and Electronics, Beijing 100049, Hefei 230026, People's Republic of China
- ^b Also at Ankara University, 06100 Tandogan, Ankara, Turkey
- ^c Also at Bogazici University, 34342 Istanbul, Turkey
- ^d Also at the Moscow Institute of Physics and Technology, Moscow 141700, Russia
- ^e Also at the Functional Electronics Laboratory, Tomsk State University, Tomsk, 634050, Russia
- ^f Also at the Novosibirsk State University, Novosibirsk, 630090, Russia
- ^g Also at the NRC "Kurchatov Institute", PNPI, 188300, Gatchina, Russia
- ^h Also at University of Texas at Dallas, Richardson, Texas 75083, USA
- ⁱ Also at Istanbul Arel University, 34295 Istanbul, Turkey

We present a measurement of the azimuthal asymmetries of two charged pions in the inclusive process $e^+e^- \rightarrow \pi\pi X$. These asymmetries can be attributed to the Collins fragmentation function, which describes the behavior of a hadron produced from a transversely polarized quark. This work is performed using a data set of 62 pb^{-1} at the center-of-mass energy $\sqrt{s} = 3.65 \text{ GeV}$ collected with the BESIII detector at the BEPCII storage rings, where the corresponding four-momentum transfer of the virtual photon, Q^2 , is close to the energy scale of the existing semi-inclusive DIS experimental data. We observe a nonzero asymmetry, which increases with increasing pion momentum and also

indicates a larger spin-dependent Collins effect than at higher energy scale. The dependence of the asymmetry on the transverse momentum of hadrons to the reference axis is also investigated. The measured asymmetries are important inputs for the global analysis of extracting the quark transversity distribution inside the nucleon, and are valuable to explore the energy evolution of the spin-dependent fragmentation function.

PACS numbers: 13.88.+e, 13.66.Bc, 13.87.Fh, 14.65.Bt

The quark-hadron fragmentation process is parameterized with a fragmentation function (FF), which describes the probability that a hadron carrying a fraction of the parton energy is found in the hadronization debris of the fragmenting parton. The Collins FF, which considers the spin-dependent effects in fragmentation processes, was first discussed by Collins in Ref. [1]. It connects the transverse quark spin with a measurable azimuthal asymmetry (the so-called Collins effect) in the distribution of hadronic fragments along the initial quark's momentum.

The measurement of the Collins FF provides an important test in understanding strong interaction dynamics and thus is of fundamental interest in understanding QCD, the underlying theory of the strong interaction. Due to its chiral-odd nature, it needs to couple to another chiral-odd function to form accessible observables in experiments. The HERMES experiment [2] presented the first non-zero measurement of this function in the semi-inclusive deep inelastic scattering (SIDIS) process by investigating the azimuthal asymmetry, where the Collins FF couples to the chiral-odd transversity [3–5] distribution. Transversity corresponds to the tensor charge of the nucleon and is the least known leading-twist quark distribution function. Subsequently, there were other SIDIS measurements of this asymmetry from HERMES [6], COMPASS [7] and JLab [8]. Direct information on the Collins FF can be obtained from e^+e^- annihilation experiments, as suggested in Ref. [9]. Measurements performed by the Belle [10–12] and BABAR [13] Collaborations give consistent non-zero asymmetries. Based on the universality of the involved functions in e^+e^- and SIDIS [14] experiments, global analyses [15, 16] have been performed to simultaneously extract the transversity and Collins functions. However, the e^+e^- Collins asymmetries taken from Belle and BABAR correspond to considerably higher Q^2 ($\approx 100 \text{ GeV}^2$) than the typical energy scale of the existing SIDIS data (mostly $2\text{--}20 \text{ GeV}^2$). Therefore, the energy evolution of the Collins FF at different Q^2 is a key factor to evaluate the uncertainty of the extracted transversity [17]. The BESIII experiment [18] studies e^+e^- annihilations at a moderate energy scale ($4\text{--}20 \text{ GeV}^2$). The authors of Refs. [19, 20] predict that the Collins asymmetry at BESIII will be larger than that at the B factories. With the comparison to the measurements from the B factories, BESIII data will help to understand the Q^2 evolution of the Collins FF. In addition, since the energy scales are very close, the BESIII data can be connected more directly to the SIDIS data.

In this Letter, we present the measurement of az-

imuthal asymmetries in pion-pion correlations for inclusive charged pion pair production in the process $e^+e^- \rightarrow \pi\pi X$, which can be attributed to the Collins effect. The analysis is based on a data sample with an integrated luminosity of 62 pb^{-1} collected with the BESIII detector [18] at the center-of-mass energy $\sqrt{s} = 3.65 \text{ GeV}$. The BESIII detector is a general-purpose solenoidal detector located at the BEPCII e^+e^- storage rings [21]. The detector has a geometrical acceptance of 93% of the full solid angle. The apparatus relevant to this work includes, from the interaction point to the outside parts, a small-cell main drift chamber (MDC) to measure momenta and specific ionizations of charged particles, a time-of-flight (TOF) system based on plastic scintillators that determines the flight time of charged particles, a CsI(Tl) electromagnetic calorimeter (EMC) detecting electromagnetic showers. These components are all situated inside a superconducting solenoid magnet that provides a 1.0 T magnetic field parallel to the beam direction. The momentum resolution for charged tracks in the MDC is 0.5% for a momentum of $1 \text{ GeV}/c$. The energy resolution for showers in the EMC is 2.5% (5.0%) for 1 GeV photons in the barrel (end cap) region. More details on the features and capabilities of the BESIII detector can be found in [18].

High statistics Monte Carlo (MC) simulated events, which are processed with a full GEANT4-based [22] simulation of the BESIII detector geometry and responses, are used to optimize the event selection criteria and check for systematics. The MC samples for light quarks in $e^+e^- \rightarrow q\bar{q}$ ($q = u, d, s$) processes are generated by the LUARLW [23] package, which is based on the Lund model but is tuned to better simulate hadronic final states in the BEPCII energy region. More MC samples including QED processes ($e^+e^- \rightarrow l^+l^-$ ($l = e, \mu, \tau$), $e^+e^- \rightarrow \gamma\gamma$), two photon fusion ($e^+e^- \rightarrow e^+e^-X$), line-shape tail production of $\psi(2S)$ and initial state radiative (ISR) process $e^+e^- \rightarrow \gamma J/\psi$ are analyzed to identify possible backgrounds.

Taking into account the spin of the quark, the number density $D_h^{q\uparrow}$ for finding a spinless hadron h with transverse momentum \mathbf{P}_h^\perp produced from a transversely polarized quark q with spin \mathbf{S}_q can be described in terms of the unpolarized FF, D_1^q , and the Collins FF, $H_1^{\perp q}$, at the leading twist [24],

$$D_h^{q\uparrow}(z, \mathbf{P}_h^\perp) = D_1^q(z, \mathbf{P}_h^{\perp 2}) + H_1^{\perp q}(z, \mathbf{P}_h^{\perp 2}) \frac{(\hat{\mathbf{k}} \times \mathbf{P}_h^\perp) \cdot \mathbf{S}_q}{zM_h}, \quad (1)$$

where $\hat{\mathbf{k}}$ denotes the direction of motion of the initial

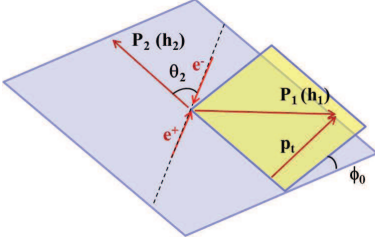


FIG. 1. The angle ϕ_0 is defined as the angle between the plane spanned by the beam axis and the momentum of the second hadron (P_2), and the plane spanned by the transverse momentum p_t of the first hadron relative to the second hadron. The angle θ_2 is the polar angle of the second hadron.

quark q , $z = 2E_h/Q$ denotes the fractional energy of the hadron relative to half of $Q = \sqrt{s}$, and M_h is the hadron mass. The second term contains the Collins function and depends on the spin orientation of the quark q , which leads to a $\sin\phi$ modulation, where ϕ is defined as the angle spanned by the transverse momentum of hadron and the plane normal to the quark spin.

In the inclusive hadron production process, $e^+e^- \rightarrow q\bar{q} \rightarrow hX$, with unpolarized beams, studies of the azimuthal asymmetries of single (anti-)quark fragmentation are impossible due to the impossibility to determine the specific (anti-)quark spin. However, the Collins effect can be observed when the fragments of the quark and anti-quark are considered simultaneously. The correlation of quark and anti-quark Collins functions gives a cosine modulation of the distribution with two times the azimuthal angle of the two hadrons, with the azimuthal angle ϕ_0 defined as the angle between the plane spanned by the beam axis and the momentum of the second hadron (P_2), and the plane spanned by the transverse momentum p_t of the first hadron relative to the second hadron, as shown in Fig. 1.

The normalized dihadron yield is recorded as a function of ϕ_0 and can be parameterized as $a \cos(2\phi_0) + b$, with b referring to the term which is independent of ϕ_0 , and a can be written as [9, 25]

$$a(\theta_2, z_1, z_2) = \frac{\sin^2 \theta_2}{1 + \cos^2 \theta_2} \frac{\mathcal{F}(H_1^\perp(z_1)\bar{H}_1^\perp(z_2)/M_1M_2)}{\mathcal{F}(D_1(z_1)\bar{D}_1(z_2))}, \quad (2)$$

where \mathcal{F} denotes a convolution over the transverse hadron momenta. M_1 and M_2 are the masses of the two hadrons, z_1 and z_2 are their fractional energies, and θ_2 is the polar angle of the second hadron with respect to the beam axis. D_1 and \bar{H}_1^\perp denote FFs for anti-quarks.

We reconstruct charged tracks from hits in the MDC. We require the polar angle to satisfy $|\cos\theta| < 0.93$, and the point of closest approach to the interaction vertex of e^+e^- is required to be within 1 cm in the plane transverse to the beam line and within 10 cm along the beam axis. Particle identification for charged tracks is accomplished by combining the measured energy loss (dE/dx) in the MDC and the flight time obtained from the TOF to de-

termine a probability $\mathcal{L}(h = K, \pi, p, e)$ for each particle (h) hypothesis. The π^\pm candidates are required to satisfy $\mathcal{L}(\pi) > 0.001$, $\mathcal{L}(\pi) > \mathcal{L}(K)$ and $\mathcal{L}(\pi) > \mathcal{L}(p)$. Photons are reconstructed from isolated clusters in the EMC, whose energies are required to be larger than 25 MeV in the EMC barrel region ($|\cos\theta| < 0.8$) and 50 MeV in end caps ($0.84 < |\cos\theta| < 0.92$). It is required that the cluster timing delay from the reconstructed event start time does not exceed 700 ns in order to suppress electronic noise and energy deposits unrelated to the event. To select inclusive $e^+e^- \rightarrow \pi\pi X$ events, at least three charged tracks are required in order to strongly suppress two body decays. At least two of the charged tracks should be identified as pions. To suppress QED backgrounds with the final state $\tau^+\tau^-$ and un-physical backgrounds, *e.g.* beam-gas interactions, the visible energy in the detector, which is defined as the total energy of all reconstructed charged tracks and photons, is required to be larger than 1.5 GeV and no electron must be present in the event, where the electron is identified with the requirement on $\mathcal{L}(e) > 0.001$ and the ratio $\mathcal{L}(e)/(\mathcal{L}(e) + \mathcal{L}(\pi) + \mathcal{L}(K)) > 0.8$. Studies based on MC samples indicate that the backgrounds are suppressed to a negligible level, less than 2.5%. We select pion pairs with $z_{1(2)} \in [0.2, 0.9]$, where the lower bound is used to reduce pions originated from resonance decays (mostly ρ, f), and the upper bound is used to reject two body decays. Compared to measurement at higher energy scale [10, 13], there is no clear jet event shape at BESIII which could help to separate the hadrons coming from different fragmenting (anti-)quark. Instead, to select back-to-back pions, we require the opening angle of the two charged pion candidates to be larger than 120° . This requirement reduces the possibility that two pions come from the fragmentation of the same quark. We label the two pions randomly as h_1 and h_2 , and we use the momentum direction of h_2 as reference axis. If more than two pions are present in an event, they are combined to each other, which means each pion is allowed to be assigned to different pion pairs.

We introduce the $2\phi_0$ normalized ratio, $R = \frac{N(2\phi_0)}{\langle N_0 \rangle}$, where $N(2\phi_0)$ is the dipion yield in each ($2\phi_0$) subdivision, and $\langle N_0 \rangle$ is the averaged bin content. The normalized ratios are built for unlike-sign ($\pi^\pm\pi^\mp$), like-sign ($\pi^\pm\pi^\pm$) and all pion-pairs ($\pi\pi$), defined as R^U , R^L and R^C , respectively, in which different combinations of favored FFs and disfavored FFs are involved. A favored fragmentation process refers to the fragmentation of a quark into a hadron containing a valence quark of the same flavor, for example $u(\bar{d}) \rightarrow \pi^+$, while the corresponding $u(\bar{d}) \rightarrow \pi^-$ is a disfavored process. Since the normalized ratio R is strongly affected by detector acceptance, we use double ratios $R^U/R^{L(C)}$ (UL and UC ratios) [10, 11] to extract the azimuthal asymmetries. Through the double ratios, charge-independent instrumental effects cancel out, and QCD radiative effects are negligible at the first order, while the charge-dependent Collins asymmetries are kept. The double ra-

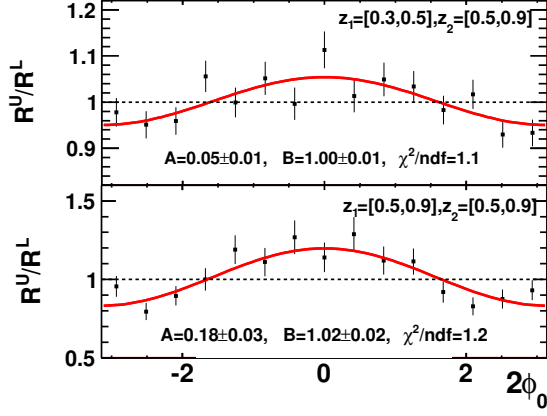


FIG. 2. Double ratio R^U/R^L versus $2\phi_0$ in the bin $z_1 \in [0.3, 0.5]$, $z_2 \in [0.5, 0.9]$ (top) and bin $z_1 \in [0.5, 0.9]$, $z_2 \in [0.5, 0.9]$ (bottom). The solid lines show the results of the fit.

ratio $R^U/R^{L(C)}$ follows the expression

$$\frac{R^U}{R^{L(C)}} = A \cos(2\phi_0) + B, \quad (3)$$

where A and B are free parameters. B should be consistent with unity, and A mainly contains the Collins effect. The A_{UL} , A_{UC} are used to denote the asymmetries for UL and UC ratios, respectively.

The analysis is performed in (z_1, z_2) bins with boundaries at $z_i = 0.2, 0.3, 0.5$ and 0.9 ($i = 1, 2$), where complementary off-diagonal bins (z_1, z_2) and (z_2, z_1) are combined. In each (z_1, z_2) bin, normalized rates $R^{U,L,C}$ and double ratios $R^U/R^{L,C}$ are evaluated in 15 bins of constant width in the $2\phi_0$ angles. In Fig. 2, the distributions of the double ratio R^U/R^L are shown for two highest (z_1, z_2) bins with the fit results using Eq. 3. In Fig. 3, the asymmetry values (A) obtained from the fit are shown as a function of six symmetric (z_1, z_2) bins. Studying the dependence on p_t is valuable for investigating the transverse momentum dependent evolution of the Collins function. The expected behavior of the Collins asymmetries as a function of $\sin^2\theta_2/(1 + \cos^2\theta_2)$ is linear (see Eq. 2). Therefore, the Collins asymmetries are investigated also in bins of p_t and $\sin^2\theta_2/(1 + \cos^2\theta_2)$, as shown in Fig. 4 and Fig. 5. The numerical results in each (z_1, z_2) and p_t bins are listed in Table I. Since one pion is allowed to be assigned to different pion pairs, the statistical uncertainties are expected to be underestimated. This is checked by repeating the whole procedure but allowing each pion to be only involved in one pion pair. We find that the statistical uncertainty in each bin becomes slightly larger, and we therefore scale the statistical errors by a factor of 1.1 for all bins.

Several potential sources of systematic uncertainties are investigated. An important test of the analysis method is the extraction of double ratios from MC samples, in which the Collins asymmetries are not included but radiative gluon and detector acceptance effects are

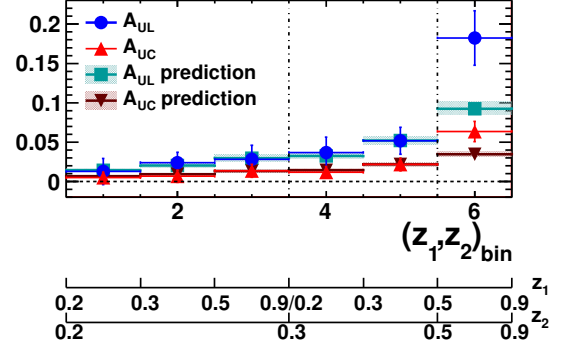


FIG. 3. Asymmetries as a function of fractional energies (z_1, z_2) for the UL (dots) and UC (triangles) ratios. The lower scales show the boundaries of the bins in z_1 and z_2 . Theoretical predictions from the authors of Ref. [20] are overlaid, where the hatched areas show the predicted bands and the points show the center values.

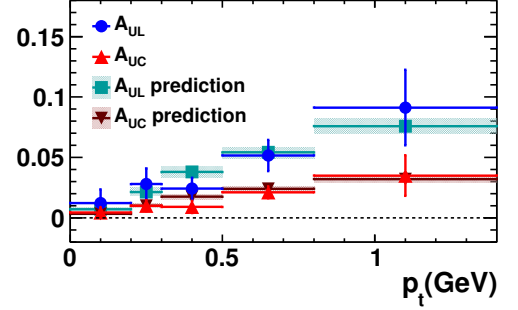


FIG. 4. Asymmetries as a function of p_t for UL (dots) and UC (triangles) ratios, where the p_t refers to the transverse momentum of the first hadron relative to the second hadron, as shown in Fig. 1. Theoretical predictions from the authors of Ref. [20] are shown using the hatched bands and the corresponding points shows the center values.

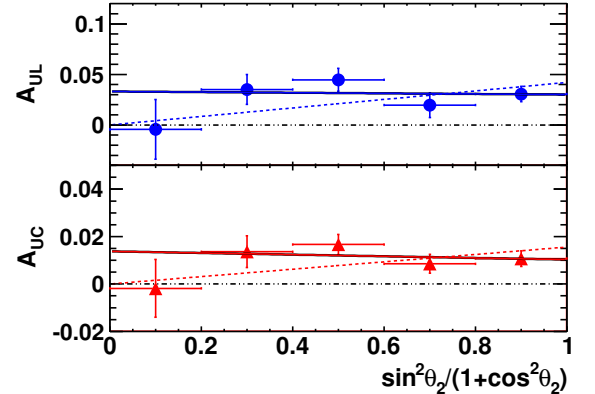


FIG. 5. Asymmetries as a function of $\sin^2\theta_2/(1 + \cos^2\theta_2)$ for UL (dots) and UC (triangles) ratios. Linear fits with the constant term being set to zero (dashed line) or a free parameter (solid line) are shown.

taken into account. The gluon radiation may induce a $\cos(2\phi_0)$ modulation according to Ref. [25], but it does not depend on the charge of the pions and is highly suppressed at the BESIII energy scale. In the MC samples, double ratios are found to be consistent with zero in all bins within statistical uncertainties. In addition, to test any potential bias in the reconstruction of the azimuthal asymmetries, MC samples are reweighted to produce generated asymmetries of 10% for UL ratios and 5% for UC ratios. The differences of reconstructed asymmetries to the input asymmetries, which are 1.0% for UL ratios and 0.6% for UC ratios on average, are included in the systematic uncertainties.

The probability of misidentifying kaons as pions may introduce $K\pi$ pairs and KK pairs into the $\pi\pi$ samples of interest. However, due to the much lower inclusive production cross section for charged kaons compared to pions, the $\pi\pi$ asymmetry receives non-negligible contribution only from the $K\pi$ combination. We denote with $A^{\pi\pi}$ and $A^{K\pi}$ the corresponding Collins asymmetries in data. They can be obtained by unfolding the measurements of $A_{\text{mea.}}^{\pi\pi}$ and $A_{\text{mea.}}^{K\pi}$, where $A_{\text{mea.}}^{\pi\pi} = (1 - f_{K\pi})A^{\pi\pi} + f_{K\pi}A^{K\pi}$, $A_{\text{mea.}}^{K\pi} = (1 - f_{\pi\pi})A^{K\pi} + f_{\pi\pi}A^{\pi\pi}$, and $f_{K\pi}$ and $f_{\pi\pi}$ are the MC-determined contamination fractions. Depending on the (z_1, z_2) bin, $f_{K\pi}$ is found to range from 0.0% to 4.5%. The corresponding changes from the nominal measured asymmetries, which vary in (0.1, 0.5)% for UL ratios and (0.0, 0.1)% for UC ratios, are assigned as systematic uncertainty.

Instrumental and gluon radiation effects are eliminated by the double ratios. Any additional contribution from gluon radiation can be examined by subtracting the normalized yields, $R^U - R^{L(C)}$. The subtraction method will cancel all the radiative terms, but the cancellation of the acceptance effects may be incomplete. The differences between the asymmetries obtained with the subtraction method and the nominal results range from 0.1% to 2.2% for UL ratios and from 0.0% to 0.5% for UC ratios. These are assigned as systematic uncertainties.

In summary, we perform a measurement of the azimuthal asymmetry in the inclusive production of charged pion pairs, which can be attributed to the product of a quark and an anti-quark Collins function. Our results suggest nonzero asymmetries in the region of large fractional energy z and indicate larger spin-dependent Collins effect than those at higher energy scale [10–13]. This is the first measurement of the Collins asymmetries at low energy scale ($Q^2 \approx 13 \text{ GeV}^2$) in an e^+e^- collider experiment. The results are of great importance to explore the Q^2 evolution of Collins function, and extract transversity distributions in nucleon.

Additional higher harmonic terms (such as $\sin 2\phi_0$ and $\cos 4\phi_0$) are also included in the fit function to validate the robustness of the fit. The changes of the value of the cosine asymmetries, which vary in (0.0, 0.9)% for UL ratios and (0.0, 0.3)% for UC ratios, are included in the systematic uncertainties.

Possible charge-dependent acceptance effects are tested by studying the double ratio of positively charged pion pairs over negatively charged pairs. The ratio is found to be consistent with unity, which indicates that the charge-dependent effects are negligible. The whole analysis procedure is validated with a zero asymmetry test based on a sample of mixed events, in which we randomly combine two pions, each from two different events. From this test, no significant asymmetries are observed. The beam polarization may contribute to the measured asymmetries. We study the angular distribution of the $e^+e^- \rightarrow \mu^+\mu^-$ process, which is sensitive to possible beam polarization. No buildup of polarization is observed, thus its influence to this measurement is negligible. All systematic uncertainties are added in quadrature.

As illustrated in Fig. 3, the measured Collins asymmetries rise with fractional energies as expected from theoretical predictions [9]. The authors of the very recent paper Ref. [20] give the first theoretical predictions for the BESIII energy scale. Overall our measured asymmetries are compatible with those predictions, except at the largest z interval; however, with the availability of more statistics in the future a definite conclusion may be drawn. The expected behavior of the Collins asymmetries as a function of $\sin^2\theta_2/(1 + \cos^2\theta_2)$ is linear and vanishes at $\theta = 0$, as formulated in Eq. (2). Thus, we perform a linear fit ($c_0 + c_1x$) to the points in Fig. 5, with the constant term c_0 set to be zero or left as a free parameter, which gives the goodness of fit to be 1.82 or 1.26 for A_{UL} and 1.70 or 1.09 for A_{UC} respectively, which indicates the results may favor a nonzero constant term, but the significance for a nonzero c_0 is only 1.87σ for both A_{UL} and A_{UC} . The current statistics can not provide a conclusive test on whether the constant term is nonzero.

ACKNOWLEDGMENTS

The authors would like to thank D. Boer, X. D. Jiang, J. P. Ma, P. Sun and F. Yuan for helpful discussions on the theoretical aspects of the measurement. The BESIII collaboration thanks the staff of BEPCII and the IHEP computing center for their strong support. This work is supported in part by National Key Basic Research Program of China under Contract No. 2015CB856700; National Natural Science Foundation of China (NSFC) under Contracts Nos. 11125525, 11235011, 11275266, 11322544, 11335008, 11425524; the Chinese Academy of Sciences (CAS) Large-Scale Scientific Facility Program; the CAS Center for Excellence in Particle Physics

TABLE I. Results of A_{UL} and A_{UC} in each (z_1, z_2) and p_t bin. The uncertainties are statistical and systematic, respectively. The averages $\langle z_i \rangle$, $\langle p_t \rangle$ and $\frac{\langle \sin^2 \theta_2 \rangle}{(1 + \cos^2 \theta_2)}$ are also given.

$z_1 \leftrightarrow z_2$	$\langle z_1 \rangle$	$\langle z_2 \rangle$	$\langle p_t \rangle$ (GeV)	$\frac{\langle \sin^2 \theta_2 \rangle}{(1 + \cos^2 \theta_2)}$	$A_{UL}(\%)$	$A_{UC}(\%)$
[0.2, 0.3][0.2, 0.3]	0.245	0.245	0.262	0.589	$1.28 \pm 0.93 \pm 1.38$	$0.50 \pm 0.32 \pm 0.60$
[0.2, 0.3][0.3, 0.5]	0.311	0.311	0.329	0.576	$2.40 \pm 0.74 \pm 1.08$	$0.67 \pm 0.27 \pm 0.72$
[0.2, 0.3][0.5, 0.9]	0.428	0.426	0.444	0.572	$2.81 \pm 1.44 \pm 1.10$	$1.36 \pm 0.54 \pm 0.64$
[0.3, 0.5][0.3, 0.5]	0.379	0.379	0.388	0.563	$3.69 \pm 1.07 \pm 1.65$	$1.17 \pm 0.39 \pm 0.62$
[0.3, 0.5][0.5, 0.9]	0.498	0.499	0.479	0.564	$5.18 \pm 1.32 \pm 1.08$	$2.17 \pm 0.47 \pm 0.65$
[0.5, 0.9][0.5, 0.9]	0.625	0.628	0.499	0.570	$18.24 \pm 3.19 \pm 1.36$	$6.37 \pm 0.99 \pm 0.82$
p_t (GeV)	$\langle p_t \rangle$ (GeV)	$\langle z_1 \rangle$	$\langle z_2 \rangle$	$\frac{\langle \sin^2 \theta_2 \rangle}{(1 + \cos^2 \theta_2)}$	$A_{UL}(\%)$	$A_{UC}(\%)$
[0.00, 0.20]	0.133	0.291	0.348	0.574	$1.22 \pm 1.02 \pm 0.48$	$0.44 \pm 0.36 \pm 0.20$
[0.20, 0.30]	0.253	0.285	0.344	0.579	$2.79 \pm 0.89 \pm 0.93$	$1.00 \pm 0.32 \pm 0.34$
[0.30, 0.45]	0.405	0.327	0.346	0.570	$2.41 \pm 0.79 \pm 0.43$	$0.90 \pm 0.26 \pm 0.43$
[0.45, 0.80]	0.610	0.453	0.349	0.571	$5.16 \pm 0.95 \pm 0.87$	$2.11 \pm 0.41 \pm 0.27$
[0.80, 1.40]	0.923	0.646	0.334	0.584	$9.13 \pm 2.74 \pm 1.52$	$3.50 \pm 0.98 \pm 1.37$

(CCEPP); the Collaborative Innovation Center for Particles and Interactions (CICPI); Joint Large-Scale Scientific Facility Funds of the NSFC and CAS under Contracts Nos. 11179007, U1232201, U1332201; CAS under Contracts Nos. KJCX2-YW-N29, KJCX2-YW-N45; 100 Talents Program of CAS; National 1000 Talents Program of China; INPAC and Shanghai Key Laboratory for Particle Physics and Cosmology; German Research Foundation DFG under Contract No. Collaborative Research Center CRC-1044; Istituto Nazionale di Fisica Nucleare, Italy; Ministry of

Development of Turkey under Contract No. DPT2006K-120470; Russian Foundation for Basic Research under Contract No. 14-07-91152; The Swedish Research Council; U. S. Department of Energy under Contracts Nos. DE-FG02-04ER41291, DE-FG02-05ER41374, DE-FG02-94ER40823, DESC0010118; U.S. National Science Foundation; University of Groningen (RuG) and the Helmholtzzentrum fuer Schwerionenforschung GmbH (GSI), Darmstadt; WCU Program of National Research Foundation of Korea under Contract No. R32-2008-000-10155-0.

-
- [1] J. C. Collins, Nucl. Phys. B **396**, 161 (1993).
 - [2] A. Airapetian *et al.* (HERMES Collaboration), Phys. Rev. Lett. **94**, 012002 (2005).
 - [3] J. P. Ralston and D. E. Soper, Nucl. Phys. B **152**, 109 (1979).
 - [4] R. L. Jaffe and X.-D. Ji, Phys. Rev. Lett. **67**, 552 (1991).
 - [5] R. L. Jaffe and X.-D. Ji, Nucl. Phys. B **375**, 527 (1992).
 - [6] A. Airapetian *et al.* (HERMES Collaboration), Phys. Lett. B **693**, 11 (2010).
 - [7] C. Adolph *et al.* (COMPASS Collaboration), Phys. Lett. B **717**, 376 (2012).
 - [8] X. Qian *et al.* (Jefferson Lab Hall A Collaboration), Phys. Rev. Lett. **107**, 072003 (2011).
 - [9] D. Boer, R. Jakob, and P. J. Mulders, Nucl. Phys. B **504**, 345 (1997).
 - [10] R. Seidl *et al.* (Belle Collaboration), Phys. Rev. Lett. **96**, 232002 (2006).
 - [11] R. Seidl *et al.* (Belle Collaboration), Phys. Rev. D **78**, 032011 (2008).
 - [12] R. Seidl *et al.* (Belle Collaboration), Phys. Rev. D **86**, 039905(E) (2012).
 - [13] J. P. Lees *et al.* (BABAR Collaboration), Phys. Rev. D **90**, 052003 (2014).
 - [14] A. Metz, Phys. Lett. B **549**, 139 (2002).
 - [15] M. Anselmino *et al.*, Phys. Rev. D **87**, 094019 (2013).
 - [16] A. Martin, F. Bradamante, and V. Barone, Phys. Rev. D **91**, 014034 (2015).
 - [17] Z.-B. Kang, A. Prokudin, P. Sun, and F. Yuan, Phys. Rev. D **91**, 071501 (2015).
 - [18] M. Ablikim *et al.* (BESIII Collaboration), Nucl. Instrum. Meth. A **614**, 345 (2010).
 - [19] P. Sun and F. Yuan, Phys. Rev. D **88**, 034016 (2013).
 - [20] Z.-B. Kang, A. Prokudin, P. Sun, and F. Yuan, (2015), arXiv:1505.05589 [hep-ph].
 - [21] C. Zhang, Sci. China G **53**, 2084 (2010).
 - [22] S. Agostinelli *et al.* (GEANT4 Collaboration), Nucl. Instrum. Meth. A **506**, 250 (2003).
 - [23] D. M. Asner *et al.*, (2008), arXiv:0809.1869 [hep-ex].
 - [24] A. Bacchetta, U. D'Alesio, M. Diehl, and C. A. Miller, Phys. Rev. D **70**, 117504 (2004).
 - [25] D. Boer, Nucl. Phys. B **806**, 23 (2009).